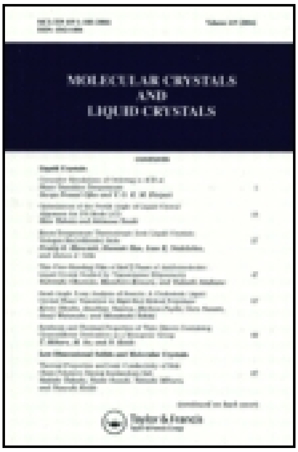

Molecular Crystals and Liquid Crystals
Publication details, including instructions for authors and subscription information:
http://www.tandfonline.com/loi/gmcl20

Optical Defect Modes in Photonic Chiral Liquid Crystals

V. A. Belyakova [a] & S. V. Semenov [b]

[a] Landau Institute for Theoretical Physics, Russian Academy of Sciences, Chernogolovka, Moscow Region

[b] Russian Research Center, “Kurchatov Institute”, Moscow, Russia

Version of record first published: 14 Jun 2011

To cite this article: V. A. Belyakova & S. V. Semenov (2011): Optical Defect Modes in Photonic Chiral Liquid Crystals, Molecular Crystals and Liquid Crystals, 543:1, 123/[889]-135/[901]

To link to this article: http://dx.doi.org/10.1080/15421406.2011.568350

Mol. Cryst. Liq. Cryst., Vol. 543: pp. 123/[889]–135/[901], 2011

ISSN: 1542-1406 print/1563-5287 online
DOI: 10.1080/15421406.2011.568350

Optical Defect Modes in Photonic Chiral Liquid Crystals

V. A. BELYAKOVA[1] AND S. V. SEMENOV[2]

[1]Landau Institute for Theoretical Physics, Russian Academy of Sciences, Chernogolovka, Moscow Region
[2]Russian Research Center, "Kurchatov Institute", Moscow, Russia

An analytic approach to the theory of the optical defect modes in chiral liquid crystals (CLC) is developed. The analytic study is facilitated by a special choice of the problem parameters. The dispersion equation determining connection of the defect mode frequency with the isotropic (defect) layer thickness is given. Analytic expressions for the transmission and reflection coefficients of the defect mode structure (CLC-defect layer-CLC) are presented and analyzed for nonabsorbing, absorbing and amplifying CLC. The effect of anomalously strong light absorption at the defect mode frequency is revealed. It is shown that in DFB lasing in a defect structure adjusting of the lasing frequency to the DM frequency results in a significant lowering of the lasing threshold. Numerical solutions of the DM dispersion equation are performed for typical values of the related parameters.

Keywords Anomalous absorption; chiral LC; localized defect modes; low threshold lasing

1. Introduction

Recently there was a very intense activity in the field of localized optical modes, in particular, defect modes in chiral liquid crystals (CLC) mainly due to the possibilities to reach a low lasing threshold for the mirrorless distributed feedback (DFB) lasing [1–4], to use the defect modes as narrow band filters [5,6] and to enhance the nonlinear optical high harmonic generation [7] in chiral liquid crystals. The defect modes existing as a localized electromagnetic eigen state with its frequency in the forbidden band gap at the structure defect were investigated initially in the three-dimensionally periodic dielectric structures [5]. The corresponding defect modes in chiral liquid crystals, and more general in spiral media, are very similar to the defect modes in one-dimensional scalar periodic structures.

They reveal abnormal reflection and transmission inside the forbidden band gap [1,2] and allow DFB lasing at a low lasing threshold [3]. The qualitative difference

Address correspondence to V. A. Belyakova, Landau Institute for Theoretical Physics, Russian Academy of Sciences, 142432, Chernogolovka, Moscow Region. Tel.: 7-499-137-32-4; E-mail: bel@landau.ac.ru; bel1937@mail.ru

with the case of scalar periodic media consists in the polarization properties. The defect mode in chiral liquid crystals is associated with a circular polarization of the electromagnetic field eigen state of the chirality sense coinciding with the one of the chiral liquid crystal helix. There are two main types of defects in chiral liquid crystals studied up to now. One of them is a plane layer of some substance differing from CLC dividing in two parts a perfect cholesteric structure and being perpendicular to the helical axes of the cholesteric structure [1]. Other one is a jump of the cholesteric helix phase at some plane perpendicular to the helical axes (without insertion any substance at the location of this plane) [2]. Recently, a lot of new types of defect layer were studied [8–14], for example, the CLC layer with the pitch differing from the pitch of two layers sandwiching the defect layer [8]. It is evident that there are many versions of the dielectric properties of the defect layer, however, the consideration below will be limited by the mentioned above two main types of defects in chiral liquid crystals.

Almost all studies of the defect modes in chiral and scalar periodic media were performed by means of a numerical analysis with the exceptions [15,16], where the known exact analytical expression for the eigen modes propagating along the helix axes [17,18] were used for a general studying of the defect mode associated with a jump of the helix phase. The used in [15,16] approach looks as a very fruitful one because it allows to reach easy understanding of the defect mode physics and it is why it deserves further implementation in the studying of the defect modes and, in particular, in specific cases allowing essential simplification of the general relationships related to the defect modes. In general, the helical media are the unique periodic structure admitting a simple exact analytic solution of Maxwell equations and, naturally, this advantage of the helical media compared to the other periodic media has to be completely exploited in solving specific boundary problems, related to the defect modes. In the present paper an analytical solution of the defect mode associated with an insertion of an isotropic layer in the perfect cholesteric structure is presented and some limiting cases simplifying the problem are considered (see also [25]).

2. Boundary Problem

To consider the defect mode associated with an insertion of an isotropic layer in the perfect cholesteric structure we have to solve Maxwell equations and a boundary problem for electromagnetic wave propagating along the cholesteric helix for the layered structure depicted at Figure 1.

As it is known [17–21] the eigenwaves corresponding to propagation of light in chiral LC along the spiral axis, i.e., the solution of the Maxwell equation

$$\frac{\partial^2 E}{\partial z^2} = c^{-2}\varepsilon(z)\frac{\partial^2 E}{\partial t^2}, \tag{1}$$

are presented by a superposition of two plane waves of the form

$$E(z,t) = e^{-\iota\omega t}[E^{+}n_{+}\exp(iK^{+}z) + E^{-}n_{-}\exp(iK^{-}z)], \tag{2}$$

where ω is the light frequency, c is the speed of light, $\varepsilon(z)$ is the CLC dielectric tensor [17–21], circular polarization vectors $n_{\pm} = (e_x \pm ie_y)/\sqrt{2}$, where e_x and e_y are

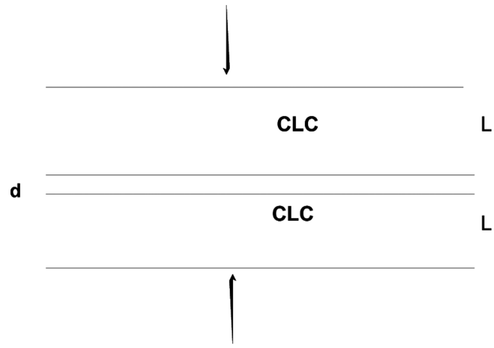

Figure 1. Schematic of the CLC defect mode structure with an isotropic defect layer.

the unit vectors along the x and y axis, and the wave vectors $K^{\pm}$ satisfy to the condition

$$K^{+} - K^{-} = \tau, \tag{3}$$

The wave vectors $K^{\pm}$ in four eigen solutions of (1) are determined by the Eq. (3) and the following formula

$$K_j^{+} = \tau/2 \pm k\{1 + (\tau/2k)^2 \pm [(\tau/k)^2 + \delta^2]^{1/2}\}^{1/2}, \tag{4}$$

where j numerates the eigen solutions and $\kappa = \omega\varepsilon_0^{1/2}c$, δ is the CLC dielectric anisotropy and $\tau = 4\pi/p$, where p is the CLC pitch. Two of the eigen waves corresponding to the circular polarization with the sense of chirality coinciding with the one of the LC spiral experience strong diffraction scattering at the frequencies in the region of the stop band. Other two eigenwaves corresponding to the opposite circular polarizations are almost not influenced by the diffraction scattering even at the frequencies of the stop band for the former circular polarization.

Because, as it is known [2,3,15,16], the specific of the defect modes in chiral LC is connected with the eigen waves of diffracting polarization we shall restrict ourselves below by the consideration of propagation of light of a diffracting polarization only due to the assumption that the average dielectric constant of the CLC ε_0 coincides with the dielectric constant of the isotropic external medium and of the isotropic layer inserted between two cholesteric layers.

We shall assume (see Fig. 1) that the chiral LC is presented by two perfect planar layer of thickness L with a spiral axes perpendicular to the layer surfaces with an insertion of an isotropic layer of thickness d between. Begin the consideration of a linear boundary problem in the formulation which assumes that two plane waves of the diffracting polarization and of the same frequency are incident along the spiral axis at the both CLC layers (see Fig. 1) from the opposite sides.

Two diffracting eigen solutions with the structure determined by Eq. (2) are excited in the both cholesteric layers. The amplitudes of the two diffracting eigenwaves denoted E_{+}^{+u} and E_{-}^{+u} for the upper and E_{+}^{+d} and E_{-}^{+u} for the bottom layer, respectively, have to satisfy to the following system of four linear equations

[20,21]

$$\begin{aligned}
&E_{+}^{+u} + E_{-}^{+u} = E_{iu} \\
&\exp[ikd]\exp[iK_{+}^{+}L_{-}]E_{+}^{+u} + \exp[ikd]\exp[iK_{-}^{+}L_{-}]E_{-}^{+u} \\
&\qquad = \exp[iK_{+}^{+}L_{+}]E_{+}^{+d} + \exp[iK_{-}^{+}L_{+}]E_{-}^{+d} \\
&\xi^{+}\exp[iK_{+}^{-}L_{-}]E_{+}^{+u} + \xi^{-}\exp[iK_{-}L_{-}]E_{-}^{+u} \\
&\qquad = \exp[ikd]\xi^{+}\exp[iK_{+}^{-}L_{+}]E_{+}^{+d} + \exp[ikd]\xi^{-}\exp[iK_{-}^{-}L_{+}]E_{-}^{+d} \\
&\qquad \exp[i2K_{+}^{-}L_{-}]\xi^{+}E_{+}^{+d} + \exp[i2K_{+} - L]\xi^{-}E_{-}^{+d} = E_{id},
\end{aligned} \tag{5}$$

where E_{iu} and E_{id} are the amplitudes of the waves of diffracting polarization incident at the cholesteric layers from the top and the bottom of the structure at Figure 1, respectively, $2L$ is the whole CLC structure thickness, d is the isotropic layer thickness, $L_{\pm} = L \pm d/2$ and

$$\begin{aligned}
&K_{\pm}^{+} = \tau/2 \pm q, \quad K_{\pm}^{-} = K_{\pm}^{+} - \tau = -\tau/2 \pm q \\
&\xi^{\pm} = \frac{E_{\pm}^{-}}{E_{\pm}^{+}} = \delta/[(K_{\pm}^{+} - \tau)^2/k^2 - 1],
\end{aligned} \tag{6}$$

where

$$q = \kappa\{1 + (\tau/2\kappa)^2 - [(\tau/\kappa)^2 + \delta^2]^{1/2}\}^{1/2}. \tag{7}$$

The frequency at the stop band centre (Bragg frequency ω_B) is given by the formula $\omega_B = 2\pi c/p\varepsilon_0^{1/2} = \tau c\varepsilon_0^{-1/2}/2$ and the band-edge frequencies $\omega_e^{\pm}$ are determined by $\omega_e^{\pm} = \omega_B/[1 - (\pm\delta)^{1/2}]$.

If one assumes E_{iu} (E_{id}) is the only nonzero amplitudes the Eq. (5) describe the reflection and transmission of light incident at the structure (Fig. 1) from above (down).

In this case the reflection and transmission coefficients of the defect structure (Fig. 1) are given via the solution of Eq. (5) by the following formulas:

$$R(d, L) = \xi^{+}E_{+}^{+u} + \xi^{-}E_{-}^{+u}, \tag{8}$$

$$T(d, L) = \exp[i(2K_{+}^{+}L + kd)]E_{+}^{+u} + \exp[i(2K_{-}^{+}L + kd)]E_{-}^{+d}, \tag{9}$$

if one assumes that only the incident from above wave exists ($E_{iu} \neq 0$, $E_{id} = 0$).

However there is another option to obtain formulas determining the optical properties of the structure depicted at Figure 1. If one use the expressions for the amplitude transmission $T(L)$ and reflection $R(L)$ coefficient for a single cholesteric layer (see also [20,21]) the transmission $|T(d, L)|^2$ and reflection $|R(d, L)|^2$ intensity coefficients for the whole structure may be presented in the following form:

$$|T(d, L)|^2 = |[T_e T_d \exp(ikd)]/[1 - \exp(2ikd)R_d R_u]|^2, \tag{10}$$

$$|R(d, L)|^2 = |\{R_e + R_u T_e T_u \exp(2ikd)/[1 - \exp(2ikd)R_d R_u]\}|^2, \tag{11}$$

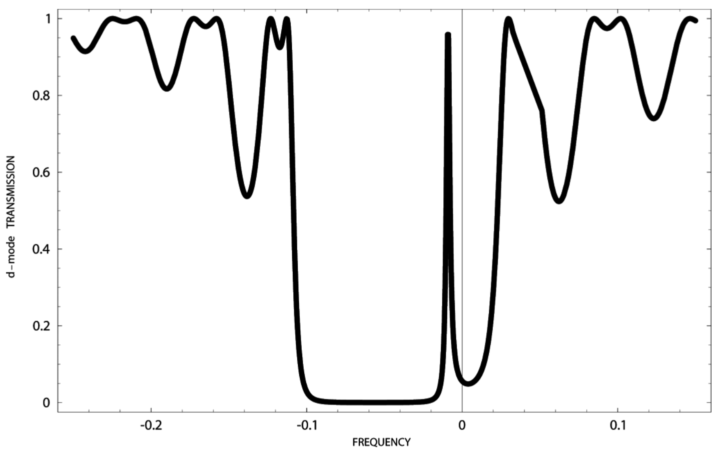

(a)

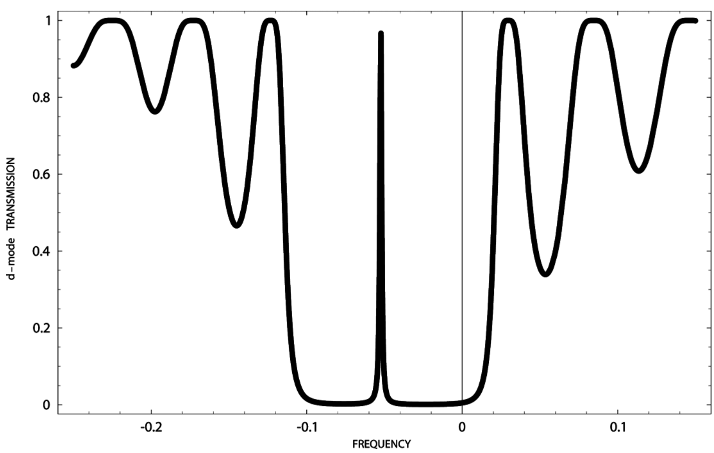

(b)

Figure 2. T(d) versus the frequency ($v/\delta = 2(\omega - \omega_0)/(\delta\omega_B) - 1$, here and at all other figures) for a nonabsorbing CLC ($\gamma = 0$) at $d/p = 0.1$ (a), $d/p = 0.25$ (b), $2\pi N = 200$, where N is the director half-turn number at the CLC layer thickness L.

where R_e (T_e), R_u (T_u), and R_d (T_d) are the amplitude reflection (transmission) coefficients of the CLC layer [25] (see Fig. 1) for the light incidence at the outer (top) layer surface, for the light incidence at the inner top CLC layer surface from the inserted defect layer and for the light incidence at the inner bottom CLC layer surface from the inserted defect layer, respectively. It is assumed in the deriving of Eqs. (10, 11) that the external beam is incident at the structure (Fig. 1) from the above only.

At Figure 2 only $T(d)$ calculated according Eq. (10) is presented because for a nonabsorbing structure $|R(d, L)^2| + |T(d, L)^2| = 1$.

3. Defect Mode

The pure defect mode (DM) is determined by Eq. (5) for $E_{iu} = E_{id} = 0$, i.e., by the solution of Eq. (5) if no waves are incident from outside at the structure depicted at Figure 1. So, the defect mode frequency ω_D is determined by zero value of the determinant of the system (5):

$$Det(d, L) = 4\{\exp(2ikd)\sin^2 qL - \exp(-i\pi L)[(\tau q/\kappa^2)\cos qL + i((\tau/2\kappa)^2 + (q/\kappa)^2 - 1)\sin qL]^2/\delta^2]\}. \quad (12)$$

Note, that the Det(d, L) at a finite thickness L does not reach zero value for a real value of ω for a nonabsorbing CLC however reaches zero alue for a complex value of ω. The larger thicknesses L of the CLC layers in the DMS structure (Fig. 1) are the smaller is the imaginary part of ω and in the limit of infinite value of L it reduces to zero in the accepted approach. So, the DM is a quasi stable mode and its life time is determined by the imaginary part of ω_D.

The solution of the homogeneous Eq. (5) allows one to find the DM field inside the CLC layers applying the expression (2) for the CLC eigen modes (see Fig. 3). For example, in an individual CLC layer of DMS (see Fig. 1) the corresponding expression for the coordinate field amplitude distribution takes the form:

$$E(\omega_D, z, t) = i\exp(-i\omega_D t)\{n_+\exp(i\tau z/2)\sin qz + (n_-/\delta)\exp(-i\tau z/2)\{[(\tau/2\kappa)^2 + (q/\kappa)^2 - 1]\sin qz - i(\tau q/\kappa^2)\cos qz\}\}, \quad (13)$$

where ω_D is the DM frequency, q is determined by Eq. (7), and $z = 0$ corresponds to the external surface of CLC layer.

4. Thick CLC Layers

In the case of DMS with thick CLC layers ($|q|L >> 1$) some analytic results related to DM can be also obtained. These results may be obtained as well from dispersion Eq. (12) so from the expressions (10, 11) for DMS transmission and reflection coefficients.

One has to admit a non zero imaginary addition to the frequency (defined, for example, by the relation $\omega/Re[\omega] = (1 + i\Delta)$, where Δ is a small quantity) and search for extremes of the Eqs. (10, 11) relative to this imaginary addition $i\Delta$.

One finds analytically the law of the life time τ_m grows with the CLC layer thickness increase, i.e., value of Δ (in the limit $|q|L >> 1$) corresponding to divergence of DMS transmission and reflection coefficients as functions of Δ, performing expansion of the denominators in Eqs. (10, 11) relative the small parameter Δ.

The corresponding expression for Δ is given by the formula

$$\Delta = \Delta q/[iqF(\delta^2)], \quad (14)$$

where Δq is the change of q due to the imaginary addition to the defect mode frequency ω_D, ensuring divergence of DMS transmission and reflection coefficients.

$$F(\delta^2) = \{1 + \{1/(2[(\tau/\kappa)^2 + \delta^2]^{1/2}) - (\tau/2\kappa)^2\}/(1 - [(\tau/\kappa)^2 + \delta^2]^{1/2} + (\tau/2\kappa)^2)\}$$

and

$$\Delta q = [2\kappa^2/(q\tau L)]\exp[-2|q|L].$$

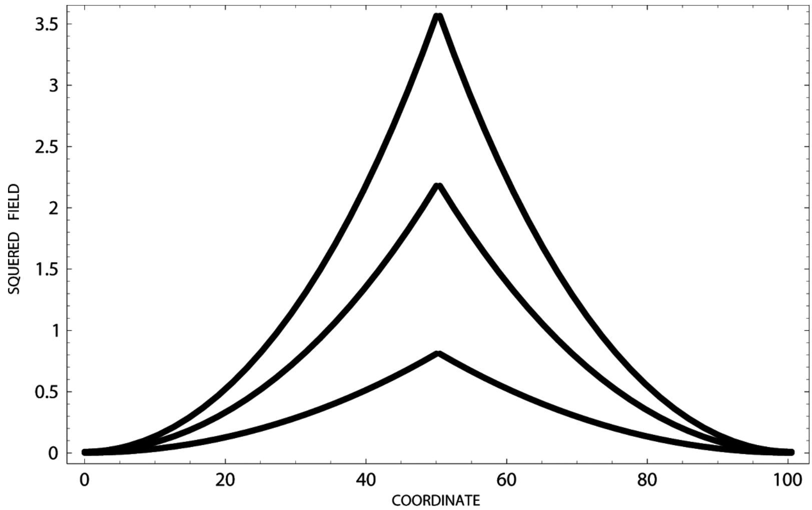

Figure 3. Coordinate dependence of the squared amplitude of the DM field (arbitrary units) at the DM frequency being at the stop band centre for various dielectric anisotropy values (from the top to the bottom $\delta = 0.05$, 0.04, 0.025) and the defect layer thickness $d = p/4$ for the cholesteric layer thickness $L = 50(p/2)$.

Because the DM life time is $\tau_m = 1/Im\omega_D$ the expression (14) reveals an exponential increase of τ_m with increase of the CLC thickness L showing also a strong dependence of the increase rate on the position of DM frequency ω_D inside the stop band. For the position of ω_D just in the middle of the stop band the expression (14) for Δ takes the following form

$$\Delta = -(2/3\pi)(p/L)\exp[-2\pi\delta(L/p)]. \tag{15}$$

The dependence of the DM lifetime on the position of ω_D inside the stop-band in the limit of thick CLC layers ($|q|L >> 1$) is shown at the Figure 4, where the results of calculations according (14) are presented for the frequency range inside the stop-band where the condition $|q|L >> 1$ holds.

5. Absorbing LC

Examine now the formulas (10, 11) for absorbing CLC layers. To take into account the absorption we define the ratio of the dielectric constant imaginary part to the real part of ε as γ, i.e., $\varepsilon = \varepsilon_0(1 + i\gamma)$. Note, that in real situations $\gamma << 1$. A natural consequence of the non zero absorption, i.e., $\gamma > 0$, is reduction of the transmission $T(d)$ and reflection $R(d)$ coefficients. However there are some interesting peculiarities of the optical properties of the structure under consideration (Fig. 1). The calculation results presented at Figure 5 reveal these peculiarities.

The total absorption $(1 - |T(d, L)|^2 - |R(d, L)|^2)$ demonstrates an unconventional frequency dependence. At a small γ for some frequencies the absorption occurs to be much more than the absorption out of the stop band (see Fig. 5). If γ is not too small (Fig. 5a, $\gamma = 0.002$) the total absorption increase reveals itself also at the stop band

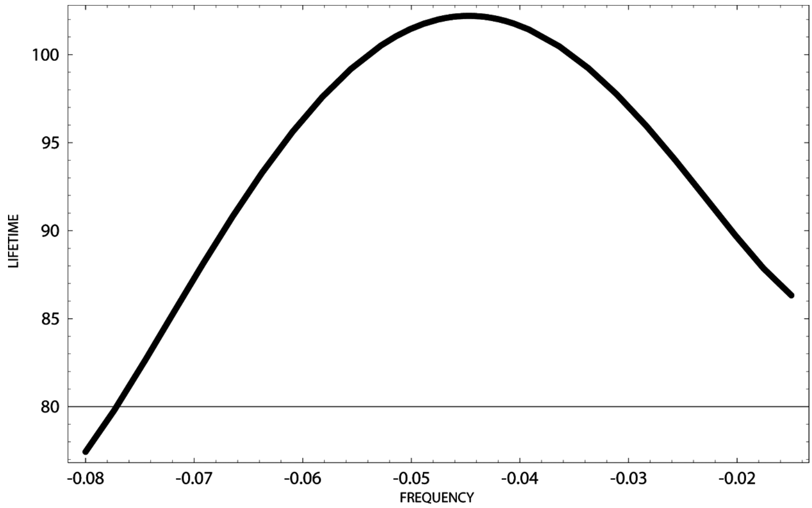

Figure 4. DM lifetime (normalized by the time of light flight throw DMS $2L\varepsilon_0^{1/2}/c$) dependence on the DM frequency ω_D location inside stop-band calculated for thick CLC layers according Eq. (14) ($\delta = 0.05$, $N = 40$, frequency of the middle point of stop-band at the figure corresponds abscissa value -0.05).

edges (at the frequencies of the stop band edge modes). It is a manifestation of the so called "anomalously strong absorption effect" known for perfect CLC layers at the edge mode frequency [20,23]. For a smaller γ (Figs. 5b) the total absorption at the defect mode frequency ω_D begins to exceed the absorption out of the stop band and at the defect mode frequency. In the case of thick CLC layers ($|q|L >> 1$) the dependence of γ, on L and other parameters ensuring maximal absorption, may be found analytically:

$$\gamma = [4\kappa^2/(q\tau L]\exp[| - 2q|L](1/iq)/\{1 + \{1/(2[(\tau/\kappa)^2 + \delta^2]^{1/2}) - (\tau/2\kappa)^2\}/(1 - [(\tau/\kappa)^2 + \delta^2]^{1/2} + (\tau/2\kappa)^2)\}. \quad (16)$$

At Figure 6 the frequency dependence of γ for a thick CLC in the limit of $|q|L \gg 1$ is presented. The Figure 6 shows that the maximal absorption enhancement occurs just in the centre of the stop band.

6. Amplifying LC

Examine the formulas (10, 11) for amplifying cholesteric layers. As above, we assume that the dielectric constant is presented by the same formula $\varepsilon = \varepsilon_0\,(1 + i\gamma)$, however with $\gamma < 0$. The calculation results for the transmission $|T(d,\ L)|^2$ and reflection $|R(d,\ L)|^2$ coefficients at $\gamma < 0$ are presented at Figure 7 and show that for a relatively small absolute value of γ a divergence of the transmission $|T(d,\ L)|^2$ and reflection $|R(d,\ L)|^2$ coefficients occurs. The corresponding value of γ may be considered as close to the threshold value of the gain (γ) for the DFB lasing at the defect mode

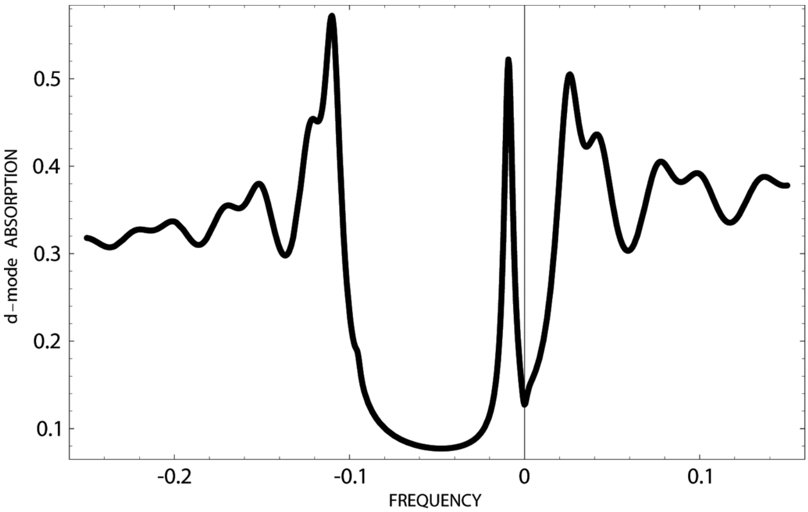

(a)

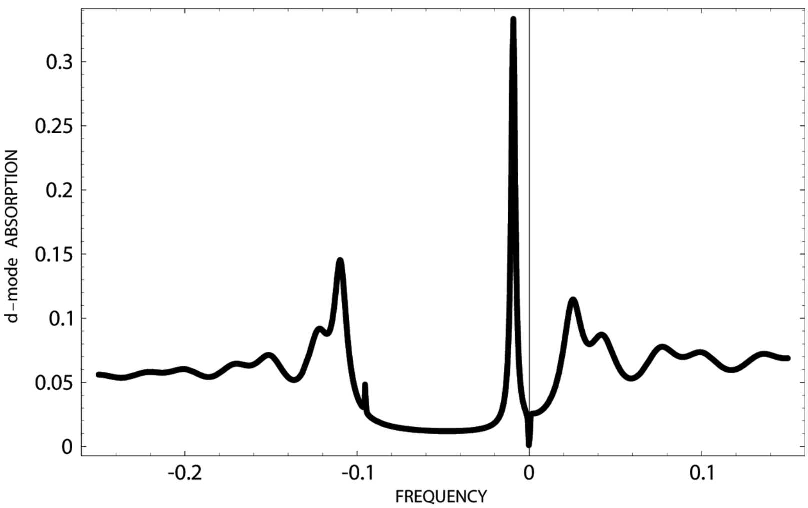

(b)

Figure 5. Total absorption $(1 - R(d) - T(d))$ for an absorbing CLC versus the frequency (a) $\gamma = 0.002$; (b) $\gamma = 0.0003$; $d/p = 0.1$, $\delta = 0.05$, $N = 33$.

frequency. To find this threshold exactly one has to solve numerically the dispersion Eq. (12).

However, in the case of thick CLC layers ($|q|L \gg 1$) the dependence of the threshold γ on L and other parameters may be found analytically similarly to the case of absorbing CLC.

For example, if the DM frequency ω_D is located at the stop band centre the corresponding interconnection for the threshold gain (γ) is given by the formula:

$$\gamma = -(4/3\pi)(p/L)\exp[-2\pi\delta(L/p)]. \tag{17}$$

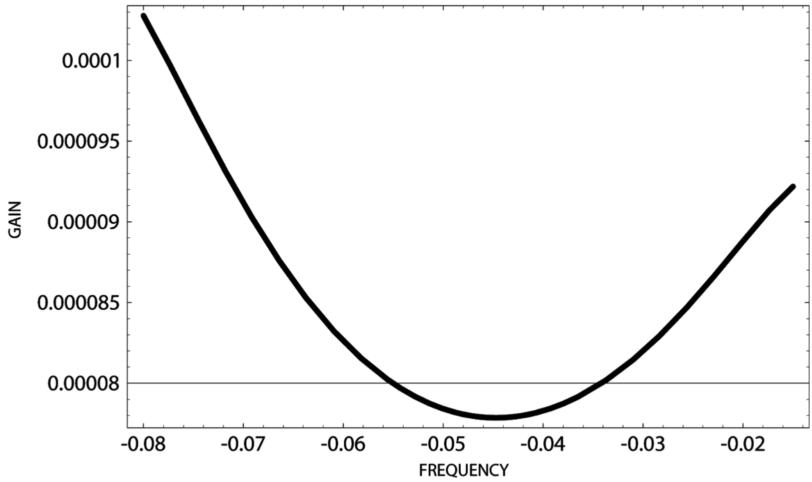

Figure 6. γ corresponding to a maximal absorption versus the DM frequency ω_D location inside stop-band is calculated for thick CLC layers according Eq. (16) ($\delta = 0.05$, $N = 40$, frequency of the middle point of stop-band at the figure corresponds the abscissa value -0.05).

7. Calculation Results

The presented above curves obtained analytically for the limiting cases may be compared with numerical calculations performed for the problem parameters corresponding to the typical their values in the experiment. The Figure 8 presents the calculated values of the DM lifetime as a function of the defect layer thickness (d/p) at the fixed CLC layers thickness L.

The Figure 9 presents the calculated values of the lasing threshold $|\gamma|$ as a function of the defect layer thickness (d/p) at the fixed CLC layers thickness L. In the

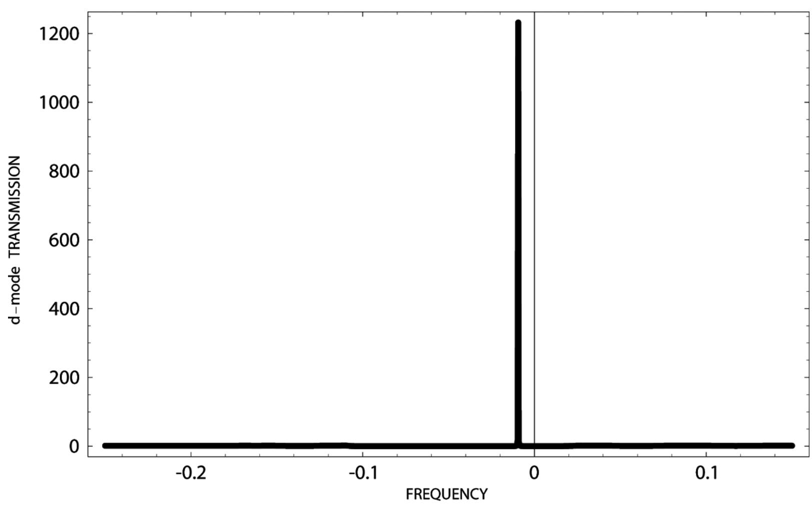

Figure 7. $T(d)$ for an amplifying CLC versus the frequency $\gamma = -0.00117$; $d/p = 0.1$, $\delta = 0.05$, $N = 33$.

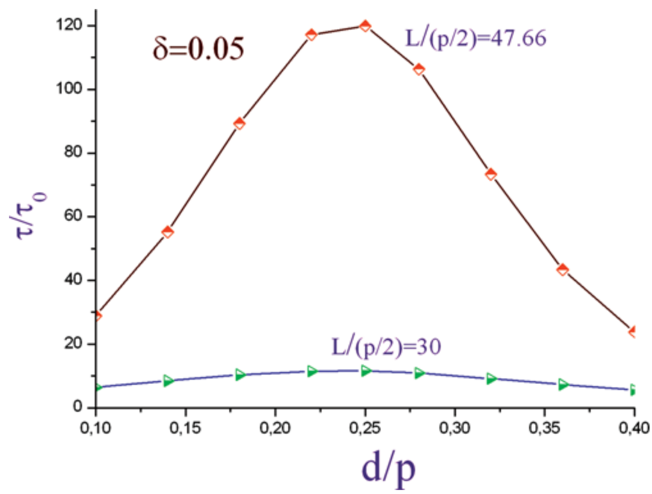

Figure 8. DM lifetime (normalized by the time of light flight throw DMS $2L\varepsilon_0^{1/2}/c$) dependence on the defect layer thickness found numerically for two values of the CLC layers thicknesses L. (Figure appears in color online.)

range of the analytical approach applicability the analytical and calculated values are in a good agreement.

8. Conclusion

The performed in the previous sections analytical description of the defect modes neglecting the polarization mixing at the boundaries of CLC in the structure under consideration allows one to reveal clear physical picture of these modes which is

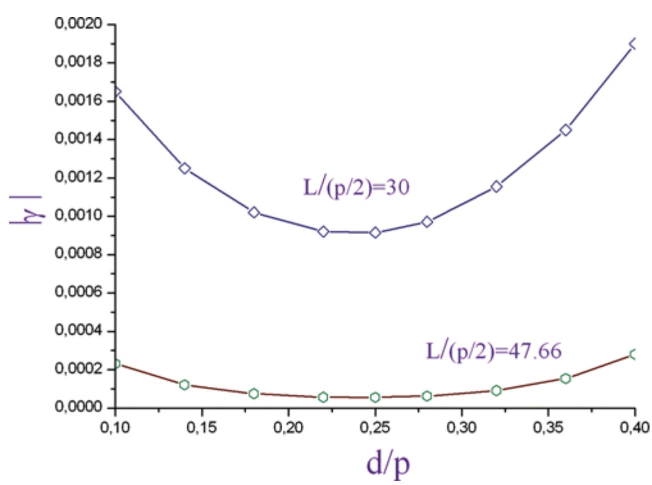

Figure 9. Lasing threshold at the DM frequency versus the defect layer thickness found numerically for two values of the CLC layers thicknesses L ($\delta = 0.05$). (Figure appears in color online.)

applicable to the defect modes in general. For example, more low lasing threshold and more strong absorption (under the conditions of anomalously strong absorption effect) at the defect mode frequency compared to the edge mode frequencies are the features of any periodic media. Note, that the experimental studies of the lasing threshold [3] agree with the corresponding theoretical result obtained above.

The defect type considered above is a homogenous layer. The developed approach is applicable also to a defect of "phase jump" type [2,3,15,16] and so the corresponding results are practically the same as above. Namely, the equation related to the case of a "phase jump" defect one gets from the equations presented above by the substitution in the factor $\exp(2ikd)$ instead of $2kd$ the quantity 2φ, where 2φ is the spiral phase jump at the defect plane.

In the conclusion should be stated that the results obtained here for the defect modes (see also [25]) and in [22,24] for the edge modes) are qualitatively applicable to the corresponding localized electromagnetic modes in any periodic media and may be regarded as a useful guide in the studies of the localized modes in general.

Acknowledgement

The work is supported by the RFBR grants 11-02-90419 Ukr_f_a and 10-02-92103-Jp_a.

References

[1] Yang, Y.-C., Kee, C.-S., Kim, J.-E., *et al.* (1999). *Phys. Rev. E*, *60*, 6852.
[2] Kopp, V. I., & Genack, A. Z. (2003). *Phys. Rev. Lett.*, *89*, 033901.
[3] Schmidtke, J., Stille, W., & Finkelmann, H. (2003). *Phys. Rev. Lett.*, *90*, 083902.
[4] Shibaev, P. V., Kopp, V. I., & Genack, A. Z. (2003). *J. Phys. Chem. B*, *107*, 6961.
[5] Yablonovitch, E., Gmitter, T. J., Meade, R. D., *et al.* (1991). *Phys. Rev Lett.*, *67*, 3380.
[6] Hodgkinson, I. J., Wu, Q. H., Torn, K. E., *et al.* (2003). *Opt. Commun.*, *184*, 57.
[7] Hoshi, H., Ishikava, K., & Takezoe, H. (2003). *Phys. Rev. E*, *68*, 020701(R).
[8] Shabanov, A. V., Vetrov, S. Ya., & Karneev, A. Yu., Pis'ma v Zhurnal Experimental'noi i Teoreticheskoi Fiziki, 80 (#3), 206, (2004) (English translation: JETP Letters, 80 (#3), 181, (2004)).
[9] Hodkinson, I. J., Wu, Q. H., Thorn, K. E., Lakhtakia, A., & McCall, M. W. (2000). *Optics Communications*, *184*, 57.
[10] Wang, F., & Lakhtakia, A. (2005). *Optics Express*, *13*(n19), 7319.
[11] Song, M. H., Ha, N. Y., Amemiya, K., Park, B., Takanishi, Y., Ishikaw, K., Wu, J. W, Nishimura, S., Toyooka, T., & Takezoe, H. (2006). *Adv. Mater.*, *18*, 193.
[12] Yoshida, H., Lee, C. H., Fuji, A., & Ozaki, M. (2006). *Appl. Phys. Lett.*, *89*, 231913.
[13] Yoshida, H., Ozaki, R., Yoshino, K., & Ozaki, M. (2006). *Thin Solid Films*, *509*, 197.
[14] Gevorgyan, A. H., & Haratyunyan, M. Z. (2007). *Phys. Rev. E*, *76*, 031701.
[15] Becchi, M., Ponti, S., Reyes, J. A., & Oldano, C. (2004). *Phys. Rev. B*, *70*, 033103.
[16] Schmidtke, J., & Stille, W. (2003). *Eur. Phys. J.*, *90*, 353.
[17] de Vries, H. (1951). *Acta Crystallogr.*, *4*, 219.
[18] Kats, E. I. (1971). *Sov. Phys. JETP*, *32*, 1004.
[19] de Gennes, P. G., & Prost, J. (1993). *The Physics of Liquid Crystals*, Clarendon Press: Oxford
[20] Belyakov, V. A., & Dmitrienko, V. E. (1989). Optics of chiral liquid crystals, p. 54 in soviet scientific reviews/Section A. In: *Physics Reviews*, Khalatnikov, I. M. (Ed.), Harwood Academic Publisher: New York, V. 13, 1–203.

[21] Belyakov, V. A. (1992). *Diffraction Optics of Complex Structured Periodic Media*, Springer Verlag: New York, Chapt. 4.
[22] Belyakov, V. A., & Semenov, S. V. (2009). *JETP*, *109*, 687; (2009). *MCLC*, *507*, 209.
[23] Belyakov, V. A., Gevorgian, A. A., Eritsian, O. S., & Shipov, N. V. (1987). *Zhurn. Tekhn. Fiz.*, *57*, 1418; (1987). *[Sov. Phys. Technical Physics*, *32*(n7), 843–845; (1988). *English translation]; Sov. Phys. Crystalography*, *33*(n3), 337.
[24] Belyakov, V. A. (2006). *MCLC*, *453*, 43; *Ferroelectrics*, *344*, 163.
[25] Belyakov, V. A. (2008). *MCLC*, *494*, 127.